Dalton Transactions

Cite this: *Dalton Trans.*, 2012, **41**, 3684

www.rsc.org/dalton

PAPER

# Study of the coordination and solution structures for the interaction systems between diperoxidovanadate complexes and 4-(pyridin-2-yl)pyrimidine-like ligands†

**Xian-Yong Yu,[a] Ping-Gui Yi,[a] Dan-Hong Ji,[a] Bi-Rong Zeng,[c] Xiao-Fang Li*[a] and Xin Xu*[b]**

***Received 3rd December 2011, Accepted 6th January 2012***
**DOI: 10.1039/c2dt12334g**



To understand the substitution effects of 4-(pyridin-2-yl)pyrimidine (pprd) on the coordination reaction equilibria, the interactions between a series of the pprd-like ligands and $[OV(O_2)_2(H_2O)]^-$ or $[OV(O_2)_2(HOD)]^-$ or $[OV(O_2)_2(D_2O)]^-$ (bpV) have been explored by a combination of multinuclear ($^1H$, $^{13}C$, and $^{51}V$) magnetic resonance, heteronuclear single quantum coherence (HSQC) and variable temperature NMR in a 0.15 mol $L^{-1}$ NaCl $D_2O$ solution that mimics physiological conditions. The direct NMR data are reported for the first time. Competitive coordination interactions result in a series of new hepta-coordinated peroxidovanadate species $[OV(O_2)_2LL']^-$ (LL′ = pprd-like chelating ligands). The equilibrium constants for the products between bpV and the pprd-like ligands show that the relative affinity of the ligands is pprd ≈ 2-$NH_2$-pprd > 2-Me-pprd > 2-Et-pprd > 4-(6-methylpyridin-2-yl) pyrimidine (abbr. 6′-Me-pprd). When the ligand is pprd, a pair of isomers (**Isomer A** and **B**) are observed in aqueous solution, which are attributed to the different types of coordination modes between the metal and the ligands, while the crystal structure of $NH_4[OV(O_2)_2(pprd)]\cdot 2H_2O$ has the same coordination structure as **Isomer A**. For substituted pprd ligands, however, only one type of structure (**Isomer A** or **B**) is observed in solution. These results demonstrate that, when the aromatic ring has a substitution group, both the steric effect (from the alkyl) and hydrogen bonding (from the amine) can affect the coordination reaction equilibrium to prevent the appearance of either **Isomer B** in solution for the ligands 2-Me-pprd, 2-$NH_2$-pprd, 2-Et-pprd, or **Isomer A** in solution for 6′-Me-pprd.

## Introduction

Heteroligand peroxidovanadate complexes, used in classical spot tests for vanadate, have received renewed attention since the 1970s due to their important biological and industrial significance.[1–4] Peroxidovanadates, as models for haloperoxidases, can oxidize hydrocarbons, alcohols and thioethers, *etc.*, under mild conditions with high selectivity and good product yields. By inhibiting protein tyrosine phosphatase (PTPase) and causing DNA cleavage both *in vitro* and *in vivo*, peroxidovanadates and complexes thereof have been tested for their potential as insulin-mimetic agents,[1–3,5] as well as for their potential as anti-tumor drugs.[6] Therefore, it is not surprising to see that the synthesis and characterization of peroxidovanadates and the study of their biological mechanisms have recently stimulated great interest.[1–12] The coordination chemistry of the peroxidovanadate complexes is also a main concern.[3,7,9–12] For example, a series of peroxidovanadate complexes containing tridentate ligands, such as nitrilotriacetic acid, were synthesized and characterized as functional models for the vanadium haloperoxidase enzymes by Pecoraro's group.[9] Based on the chemistry observed for these model compounds, they proposed a mechanism of halide oxidation. Posner *et al.* synthesized and characterized twelve peroxidovanadate complexes containing bidentate ligands, *e.g.*, oxalate, 2,2′-bipyridine (bipy) and 1,10-phenanthroline, and studied their insulinomimetic activities.[5] Shaver and co-workers synthesized peroxidovanadate complexes, including picolinate and its derivatives and studied the reactions between these complexes with cysteine.[10] Furthermore, peroxidovanadates containing other bidentate ligands, such as 2-(2-pyridyl)-imidazole or picolinamide, have been successfully synthesized by Chen's group.[11c,d] The general structures of some

[a]*Key Laboratory of Theoretical Chemistry and Molecular Simulation of Ministry of Education, Hunan Province College Key Laboratory of QSAR/QSPR, School of Chemistry and Chemical Engineering Hunan University of Science and Technology, Xiangtan 411201, China. E-mail: fine_chem@163.com; Fax: +86-731-58290509*
[b]*Shanghai Key Laboratory of Molecular Catalysis and Innovative Materials, MOE Laboratory for Computational Physical Science, Department of Chemistry, Fudan University, Shanghai, 200433; State Key Laboratory of Physical Chemistry of Solid Surfaces, College for Chemistry and Chemical Engineering, Xiamen University, Xiamen 361005, China. E-mail: xxchem@fudan.edu.cn*
[c]*Department of Materials Science and Engineering, Key Laboratory for Fire Retardant Materials of Fujian Province, Xiamen University, Xiamen 361005, China*

† Electronic supplementary information (ESI) available: the experimental procedures and spectroscopic data of ligands **1–7** and complexes **8** and **9** are summarized in the ESI. For ESI and crystallographic data in CIF or other electronic format see DOI: 10.1039/c2dt12334g

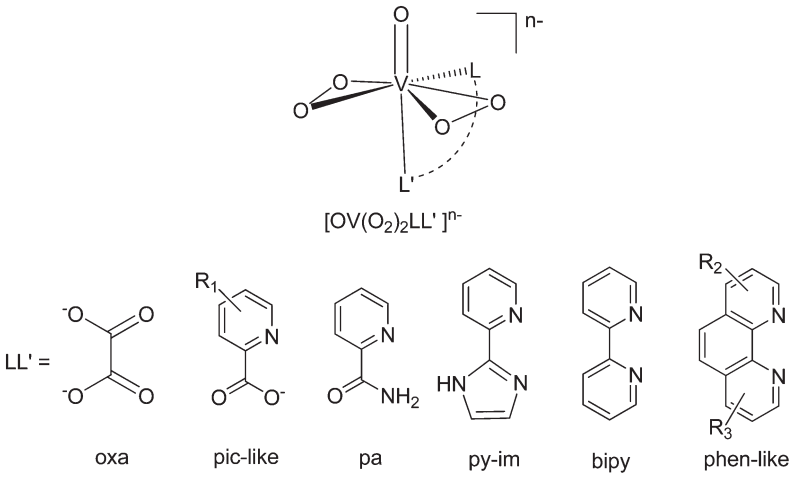


**Scheme 1** The general structures of some heteroligand (LL′) coordinated peroxidovanadate complexes.[5,10–12]

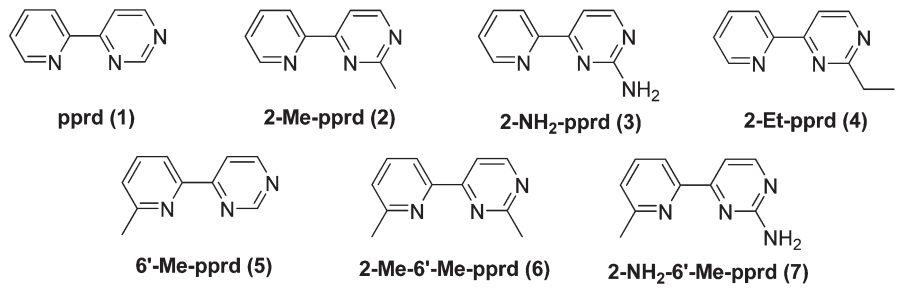


**Scheme 2** The structures of the 4-(pyridin-2-yl)pyrimidine derivatives: the pprd-like ligands **1**–**7**.

heteroligand (LL′) coordinated peroxidovanadate complexes are shown in Scheme 1. The importance to choose these chelating ligands, which contain pyridine building block in particular, for synthesizing peroxidovanadates has been demonstrated previously.[12]

The 4-(pyridin-2-yl)pyrimidine (pprd) ligand,[13] which has both the pyridine and pyrimidine rings, is analogous to bipy in terms of the chelating site and is expected to be a good ligand for the formation of peroxidovanadate complexes. At the same time, in order to probe the substitution effects on the coordination reaction equilibrium of the pprd ligand to peroxidovanadate, we have synthesized a series of the pprd-like ligands (**1**–**7**, shown in Scheme 2) and used multinuclear ($^{1}$H, $^{13}$C and $^{51}$V) magnetic resonance, heteronuclear single quantum coherence (HSQC) and variable temperature NMR to explore the interactions between $[OV(O_2)_2(H_2O)]^-$/$[OV(O_2)_2(D_2O)]^-$/$[OV(O_2)_2(HOD)]^-$ (all of which may be abbreviated to 'bpV') and the pprd-like ligands in a 0.15 mol $L^{-1}$ NaCl $D_2O$ solution that mimics physiological conditions. When the ligand was pprd (**1**) or 2-$NH_2$-pprd (**3**), two new single crystals were obtained and their structures were characterized by NMR and single crystal X-ray diffraction. Through the combined use of these methods, and by comparison with the crystal structures, solution structures and coordination modes for all species in the interacting systems were determined. A better understanding was achieved, which suggested that the coordination equilibrium in solution are influenced by both the steric effect (from the alkyl group) and the hydrogen bonding interactions (from the amine group).

## Results and discussion

### Solid state structures of 8 and 9

Both crystals of **8** and **9** consist of ammonium ions, pprd-like ligand-coordinated biperoxidovanadate(v) complexes and water, held together by ionic and hydrogen bonding interactions. The structures of $[OV(O_2)_2(pprd)]^-$ and $[OV(O_2)2(2\text{-}NH_2\text{-}pprd)]^-$ are depicted in Fig. 1, both of which share the same distorted pentagonal bipyramidal geometry. Within the limits of experimental error, the four peroxido oxygens, as well as the nitrogen atom in the pyridine ring, define an equatorial plane with respect to the axial V═O bond. A nitrogen atom in the pyrimidine ring binds to V in the axial position. Selected bond lengths of **8** and **9** are presented in Table 1, which are compared with the corresponding values of other biperoxidovanadate complexes. More detailed structural data (bond distances and angles) of **8** and **9** can be found in ESI, shown in Table S1.†

Table 1 shows that the axial V═O lengths are 1.611 Å for **8** and 1.606 Å for **9**, which are typically found for a double bond between V and O atoms and are within the range observed in similar geometries, such as those of $[OV(O_2)_2(py\text{-}im)]^-$ and $[OV(O_2)_2(im)]^-$.[3,11c] The vanadium atom displaces 0.358 (in **8**) or 0.341 Å (in **9**) from the equatorial plane, which are comparable to that of ~0.3 Å found in other seven-coordinated biperoxidovanadate complexes.[11c,14] The $V\text{–}O_{peroxido}$ bond lengths (1.878–1.912 Å) are also within the range of the normal $V\text{–}O_{peroxido}$ bond distances reported in $[OV(O_2)_2(bipy)]^-$ and

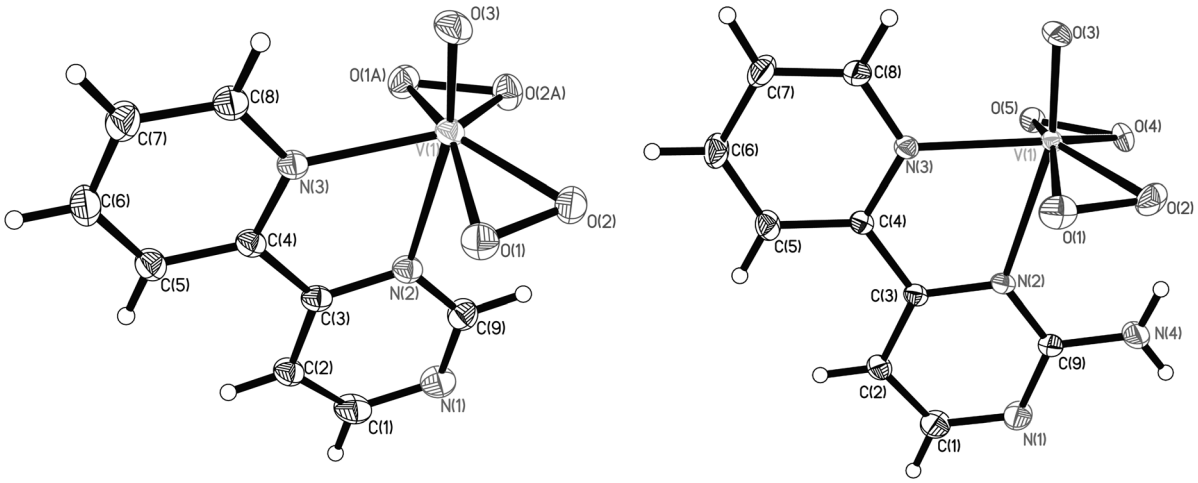


**Fig. 1** Structures of the pprd-like ligand-coordinated peroxidovanadate complexes in the $NH_4[OV(O_2)_2(pprd)]\cdot 2H_2O$ (**8**, on the left) and $NH_4[OV(O_2)_2(2\text{-}NH_2\text{-}pprd)]\cdot 3H_2O$ (**9**, on the right) crystals. Ammonium ions and the water molecules are not shown.

**Table 1** Selected bond lengths of **8** and **9**, as well as those of the other biperoxidovanadate complexes

| | **8** | **9** | bpV(im) | bpV(pic) | bpV(py-m) | bpV(bipy) |
|---|---|---|---|---|---|---|
| V═O | 1.611(3) | 1.606(3) | 1.603(2) | 1.599(4) | 1.614(2) | 1.619(3) |
| $V–O_{peroxido(trans)}$ | 1.895(2) | 1.882(4) | 1.922(2) | 1.895(4) | 1.891(2) | 1.883(3) |
| | | 1.878(4) | 1.884(2) | 1.881(4) | 1.879(2) | 1.880(3) |
| $V–O_{peroxido(cis)}$ | 1.887(2) | 1.912(4) | 1.866(2) | 1.917(4) | 1.918(2) | 1.911(3) |
| | | 1.901(3) | 1.865(2) | 1.899(4) | 1.899(2) | 1.909(3) |
| $(O–O)_{peroxido}$ | 1.472(3) | 1.473(6) | 1.475(2) | 1.464(5) | 1.462(3) | 1.471(4) |
| | | 1.465(5) | 1.467(3) | 1.458(6) | 1.449(3) | 1.465(4) |
| $V–N_{equatorial}$ | 2.142(3) | 2.128(4) | 2.092(2) | 2.123(5) | 2.102(3) | 2.149(4) |
| $V–N/O_{axial}$ | 2.332(3) | 2.400(4) | — | 2.290(4) | 2.356(3) | 2.288(3) |
| Ref. | This work | | 3 | 10 | 11*c* | 14*e* |

$[OV(O_2)_2(py\text{-}im)]^-$.[11c,14e] The lengths of the $(O–O)_{peroxido}$ bonds are around 1.465–1.472 Å, similar to the corresponding values in $[OV(O_2)_2(im)]^-$ and $[OV(O_2)_2(bipy)]^-$.[3,14e] The bond lengths for both $V–N_{equatorial}$ (2.142 Å for **8**, 2.128 Å for **9**) and $V–N_{axial}$ (2.332 Å for **8**, 2.399 Å for **9**) are in good agreement with the corresponding values reported for other peroxidovanadate complexes, such as $[OV(O_2)_2(bipy)]^-$, $[OV(O_2)_2(pic)]^-$ and $[OV(O_2)_2(py\text{-}im)]^-$.[3,10,11c,14]

Fig. 2 gives the $^{51}V$ MAS NMR spectra recorded at the spinning rates of 3, 5 and 7 kHz, where the chemical shifts of **8** and **9** are −719 and −738 ppm, respectively. This remarkable shielding difference between **8** and **9** can be naturally attributed to the electronic effects imparted by the nature of the ligands/ligand sphere. Such electronic effects also show up in the geometry differences between **8** and **9**, shown in Table 1, and the corresponding differences in the IR data presented in the ESI.†

### Solution state structures of 8 and 9

Although X-ray diffraction provides conclusive results for the coordination modes in **8** and **9** in the solid state, we are very much interested in their solution state structures, which we explored using NMR spectroscopy in solution. The details of the $^1H$ and $^{13}C$ NMR spectroscopic data for **8** and **9** in solution are presented in the ESI.†

Fig. 3 shows a comparison between the $^{13}C$ NMR spectra of **9** in solution (a) and in the solid state (b). There is a clear one to one correspondence, which provides strong evidence showing that, for the 2-$NH_2$-pprd (**3**) ligand, only one coordination mode to the metal is observed in solution, which corresponds to the same structure adopted by the crystal form of **9**. For **8** with the pprd (**1**) ligand, the comparison between the $^{13}C$ NMR spectra in solution (c) and in the solid state (d) is not so straightforward. Obviously, the signals in solution can be grouped into two sets, one stronger (labeled with *) and one weaker. We assume that when **8** is dissolved in solution, there exists a pair of isomers (**A** and **B**). While **Isomer A**, corresponding to the set of stronger signals, is the main product in solution, which may adopt the same coordination mode as that in the solid state of **8**, **Isomer B**, which corresponds to the set of weaker signals, is the minor product in solution, which may adopt a different coordination mode compared to that in the solid state. Through inspection of the crystal structure in Fig. 1, we assume that **Isomer B** may have a coordination mode with $N_{equatorial}$ and $N_{axial}$ interchanged, *i.e.*, it is the nitrogen atom in the pyridine ring, instead of that in the pyrimidine as in **Isomer A**, that binds to V in the axial position in **Isomer B**. What has led to the difference in coordination modes between complexes **8** and **9** in solutions? We will ascertain the coordination modes associated with **Isomers A** and **B** and will explore their formation mechanisms. At the same time,

 

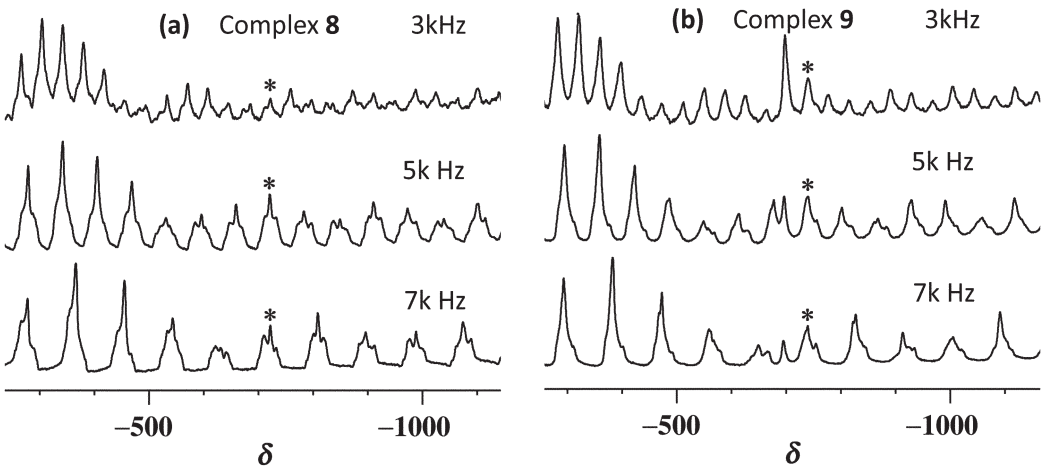


**Fig. 2** The solid-state $^{51}$V NMR spectra of **8** (a) and **9** (b). The asterisk indicates the $^{51}$V NMR signal; other bands are spinning side-bands.

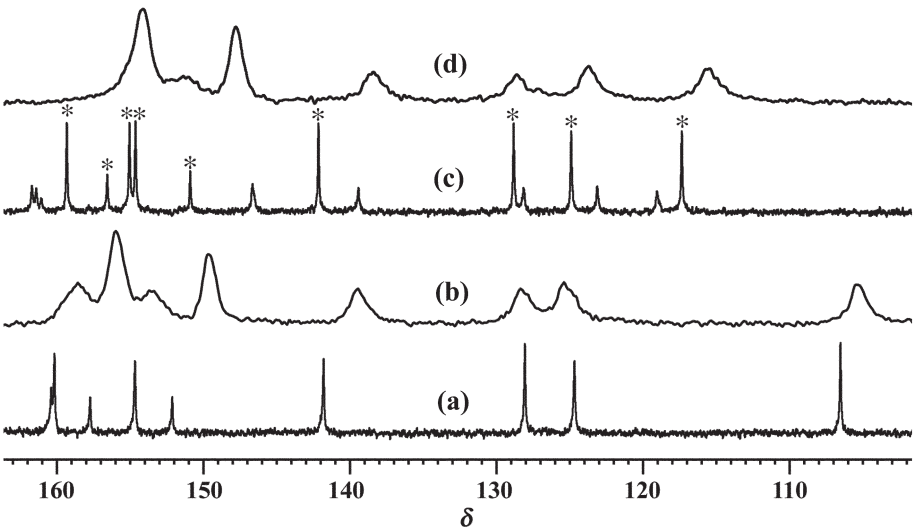


**Fig. 3** $^{13}$C NMR spectra: complex **9** in solution (a) and in the solid-state (b); complex **8** in solution (c) and in the solid-state (d).

we will discuss in the following sections the substitution effects on the coordination reaction equilibria of a series of the pprd-like ligands (**1–7**) to biperoxidovanadates.

### $^{1}$H and $^{13}$C NMR data of the interaction systems between bpV and the pprd-like ligands

In order to explore the coordination between pprd (**1**) and the vanadium metal center, the bpV–pprd interaction systems were studied using $^{1}$H and $^{13}$C NMR spectroscopy. The bpV solution was first prepared according to the procedure described in the Experimental section and then varying amounts of the pprd (**1**) ligand were added.

Fig. 4(a) shows the $^{13}$C NMR spectrum when the molar ratio of pprd (**1**) and bpV is 1 : 1. As it is clear, there exist two sets of peaks, which are identical to Fig. 3(c) for the solution complex of **8**. The set of stronger signals indicates the formation of **Isomer A**, while the weaker one is assigned to **Isomer B**. These peaks do not correspond to the free pprd ligands. When the amount of pprd (**1**) was increased (from 1 to 1.5 equivalent), the peaks of the free ligands appeared as shown in Fig. 4(b). According to the assignments of the $^{13}$C NMR signals for the bpV–pprd interaction system, the $^{1}$H NMR signals can also be assigned through the HSQC spectrum, which is displayed in Fig. 5.

The NMR results for the other interaction systems between bpV and the pprd-like ligands (**2–5**) are summarized in ESI (Table S2†). The shifts of the $^{1}$H and $^{13}$C NMR spectra as compared to those of the corresponding spectra of the free ligands suggest that ligands **2–5** indeed coordinate to bpV, whereas ligands **6** and **7** do not as no such shifts were observable. Interestingly, only pprd (**1**) displays two sets of signals, while all others show only one set of signals, suggesting all other pprd-like ligands (**2–5**) adopt a single coordination mode which is similar to the one in crystal **8** or **9** or their solution structures. These *N,N′*-chelating biheteroaromatic ligands can form the hepta-coordinated $[OV(O_2)_2LL']^-$ species as exemplified by $[OV(O_2)_2(py\text{-}im)]^-$ studied previously[11c] (*cf.* Scheme 1).

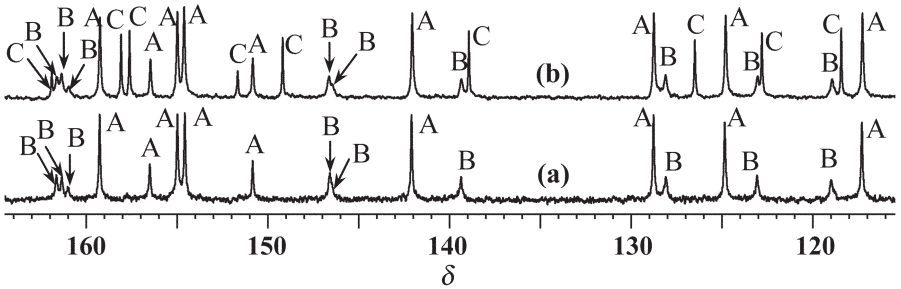


**Fig. 4** $^{13}$C NMR spectra of the bpV–pprd interaction system in aqueous solution. The molar ratio of bpV and pprd is 1 : 1 and 1 : 1.5 in (a) and (b), respectively. A, B and C label the signals from **Isomer A**, **Isomer B** and the free pprd (**1**) ligand, respectively.

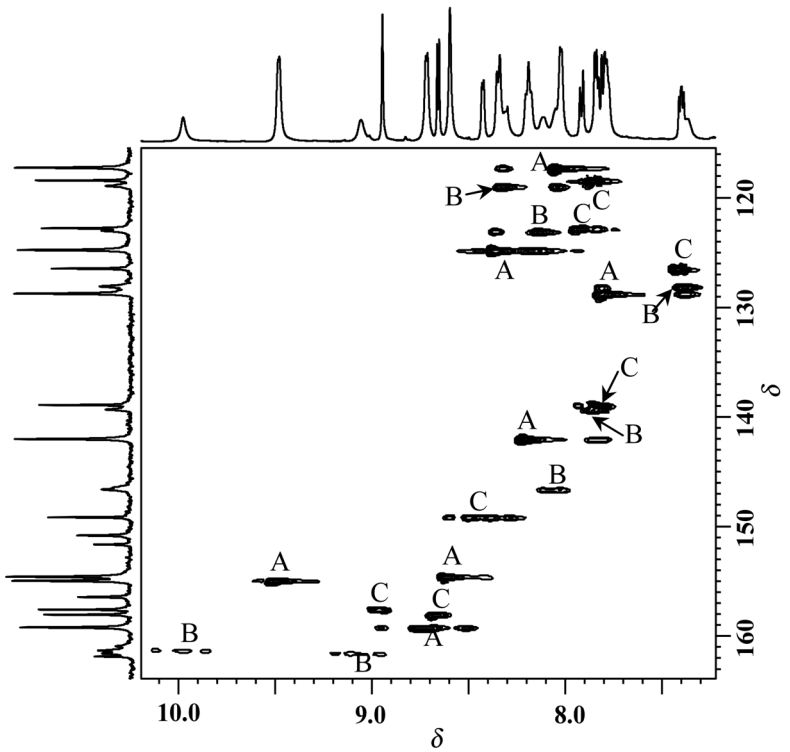


**Fig. 5** The HSQC spectrum of the bpV–pprd interaction system in aqueous solution. The molar ratio of bpV and pprd is 1 : 1.5. A, B and C label the signals from **Isomer A**, **Isomer B** and the free pprd (**1**) ligand, respectively.

### $^{51}$V NMR of the interaction systems between bpV and the pprd-like ligands

The $^{51}$V NMR results for the interaction systems between bpV and the pprd-like ligands (**1–5**) are also summarized in ESI (Table S2†). In this section, we will discuss them in detail.

It was reported that the as-prepared bpV (see Experimental section) has a $^{51}$V peak at −692 ppm as shown Fig. 6(a).[15] When pprd was added to the bpV solution, new peaks appeared at about −741 and −745 ppm (see Fig. 6(b)–(d)), which suggest the formation of the bpV–pprd complex $[OV(O_2)_2(pprd)]^-$. **Isomer A**, corresponding to the main peak, is the major product, while **Isomer B**, corresponding to the shoulder peak, is the minor product. Their intensities increase with an increase of the molar ratios of pprd–bpV (from 0 to 1, and finally to 1.5 equivalents) before reaching a maximum, as shown in Fig. 6(b)–(d). However, the molar ratio between **Isomer A** and **B** is still 2 : 1 in the process of adding pprd (**1**). These results echo the $^1$H and $^{13}$C NMR spectra of **8** in solution as well as those of the bpV + **1** system, lending further support to the suggestion that the appearance of two set of peaks for the species of $[OV(O_2)_2(pprd)]^-$ in the NMR spectra is a strong indication that there exist two types of coordination mode for the pprd ligand (**1**) binding to the metal center.

In order to explore the temperature influence on the coordination equilibrium, variable temperature $^{51}$V NMR was used to study the interaction system between bpV and pprd (**1**) in the range of 20–40 °C. The experimental results shown in Fig. 7 show that: (1) all the peaks in the spectra move towards the low field when the temperature is increased. The chemical shift of bpV moves about 5.5 ppm every 10 °C and that of $[OV(O_2)_2(pprd)]^-$ moves about 4.5 ppm every 10 °C. (2) The

 

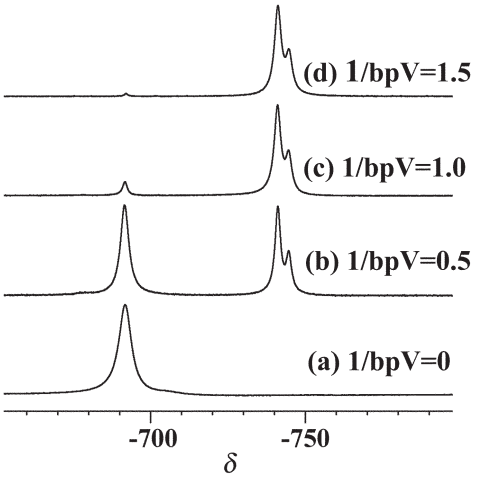


**Fig. 6** The $^{51}$V NMR spectra of the interaction system between bpV and pprd (**1**) in an aqueous solution. (a)–(d) correspond to molar ratios of pprd/bpV = 0, 0.5, 1.0 and 1.5, respectively.

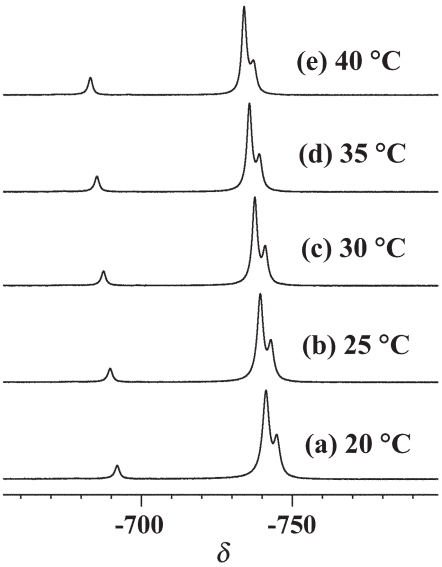


**Fig. 7** Variable temperature $^{51}$V NMR spectra of the interaction system between bpV and pprd (**1**) with a 1 : 1 molar ratio in an aqueous solution.

quantity of the $[OV(O_2)_2(pprd)]^-$ species decreases when the temperature is increased. However, the ratio between **Isomers A** and **B** is still maintained at 2 : 1 in the temperature range of 20–40 °C. This implies that, with an increase in temperature, the coordination bonds between vanadium and pprd (**1**) are weakened and both **Isomer A** and **B** are converted back to bpV gradually.

The respective $^{51}$V NMR spectra with all pprd-like ligands (**1**–**7**) are displayed in Fig. 8, which suggest how the substitution groups on the pprd ligand affect the coordination equilibrium with bpV. While the bpV peak intensity decreased, new peaks appeared as the corresponding pprd ligands were added. For 2-Me-pprd (**2**), a new peak at about −732 ppm, see Fig. 8(b), was assigned to $[OV(O_2)_2(2\text{-Me-pprd})]^-$. Similarly, new peaks shown in Fig. 8(c)–8(e) at −739, −729 and −736 ppm were

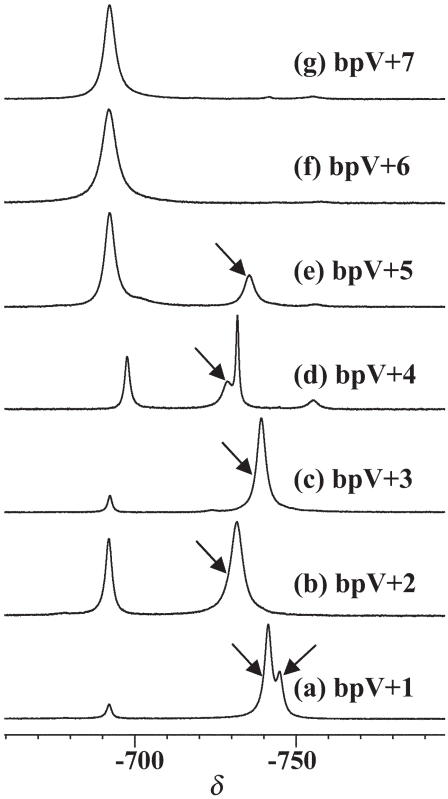


**Fig. 8** $^{51}$V NMR spectra of the interaction systems of bpV and the pprd-like ligands (**1**–**7**) in an aqueous solution. The peaks of the newly formed $[OV(O_2)_2LL']-$ (LL′ = **1**–**7**) species are indicated by arrows.

assigned to $[OV(O_2)_2(2\text{-}NH_2\text{-pprd})]^-$, $[OV(O_2)_2(2\text{-Et-pprd})]^-$, and $[OV(O_2)_2(6'\text{-Me-pprd})]^-$, respectively, for the corresponding pprd-like ligands of (**3**)–(**5**). The upfield signals may correspond to some ligand-free peroxidovanadates. For example, the small new peaks at −732 and −755 ppm in Fig. 8(d) may be assigned to $[HVO(O_2)_3]^{2-}$ and $[HV_2O_3(O_2)_4]^{3-}$, respectively, according to a previous literature report.[16] The assignment of the pprd-like ligand coordinated $^{51}$V peak can be confirmed by checking the $^{51}$V peak intensity varying with the concentration of the pprd-like ligands (see below for further discussion). As noted from Fig. 8(f) and 8(g), no new peaks appear besides those of bpV. This is an indication that 2-Me-6′-Me-pprd (**6**) or 2-$NH_2$-6′-Me-pprd (**7**) can not coordinate to bpV to form the corresponding bpV–pprd-like complexes. Therefore, based on the ratios of the bpV peak areas before and after coordination, the relative affinity of the pprd-like ligands towards bpV is deduced as **1** ≈ **3** > **2** > **4** > **5**, with **6** and **7** having no affinity.

### Quantitative measurements of the interaction systems between bpV and the pprd-like ligands

To gain a quantitative evaluation of the coordination affinity of the ligands, the equilibrium constants were determined *via* NMR studies using a procedure as described by Tracey *et al.*[7] Note that bpV here stands for $[OV(O_2)_2(H_2O)]^-$. Hence, when a pprd ligand is coordinated to bpV, it is actually a substitution reaction:

$$\text{bpV} + \text{pprd} - \text{like} \rightarrow \text{bpV}(\text{pprd} - \text{like}) + H_2O \qquad (1)$$

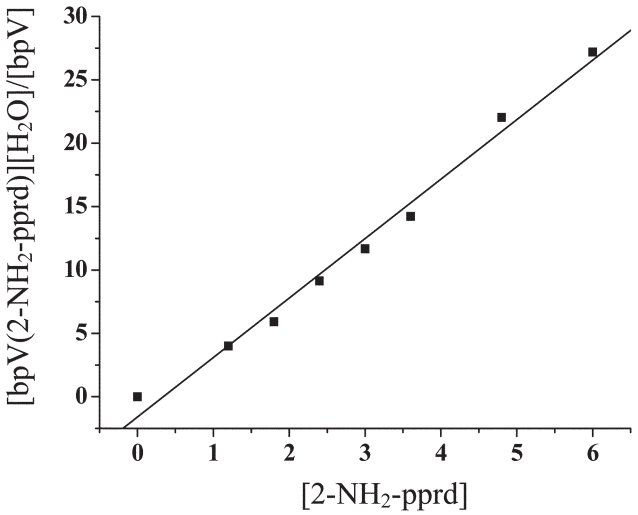


**Fig. 9** Determination of the equilibrium constant for the coordination between bpV and the 2-$NH_2$-pprd (**3**) ligand according to eqn. (2). Conditions of the experiments: temperature 25 °C, 15.0 mmol $L^{-1}$ total vanadate, 0.6 mol $L^{-1}$ KCl, 20 mM HEPES buffer (pH 6.8) and varying amounts of 2-$NH_2$-pprd (0.0–6.0 mmol $L^{-1}$).

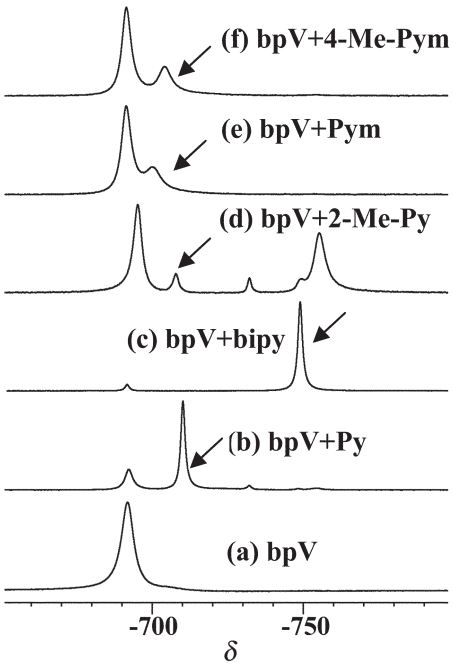


**Fig. 10** $^{51}V$ NMR spectra of the interaction systems between bpV and the pyridine-like (pyridine is abbreviated to Py; 2,2-bipyridine is abbreviated to bipy; 2-methylpyridine is abbreviated to 2-Me-Py) or pyrimidine-like (pyrimidine is abbreviated to Pym; 4-methylpyrimidine is abbreviated to 4-Me-Pym) ligands in an aqueous solution. The total concentration of the vanadate species is 0.2 mol $L^{-1}$. The peaks of the newly formed species, $[OV(O_2)_2L'']^-$ (L″ = Py, bipy, 2-Me-Py, Pym or 4-Me-Pym), are indicated by arrows.

**Table 2** The equilibrium constants for the coordination between bpV and the pprd-like ligands as determined *via* $^{51}V$ NMR studies using a procedure described by Tracey *et al.*[7] Note that the linear correlation coefficient, *R*, is generally higher than 0.99

| | bpV + pprd-like = $[OV(O_2)_2(\text{pprd-like})]^- + H_2O$ | | |
|---|---|---|---|
| Ligand | $\delta$ ($^{51}V$) | *K* | *R* |
| pprd (**1**) | −741, −745 | $4.4 \times 10^3$ | 0.9907 |
| 2-Me-pprd (**2**) | −732 | $1.8 \times 10^3$ | 0.9987 |
| 2-$NH_2$-pprd (**3**) | −741 | $4.7 \times 10^3$ | 0.9939 |
| 2-Et-pprd (**4**) | −731 | $9.5 \times 10^2$ | 0.9966 |
| 6′-Me-pprd (**5**) | −734 | 83 | 0.9925 |

Based on eqn. (1), the equilibrium constants of various coordination reactions could be calculated according to eqn. (2):

$$K = [\text{bpV}(\text{pprd} - \text{like})][H_2O]/[\text{bpV}][\text{pprd} - \text{like}] \quad (2)$$

where, in an aqueous solution, the concentration of water is just a constant. Fig. 9 plots the ratio change of [bpV(pprd-like)]/[bpV] with varying [pprd-like] when the pprd-like ligand is 2-$NH_2$-pprd (**3**), where the slope corresponds to its equilibrium constant *K*. The constants, *K*, for the other pprd-like ligands can be measured in the same way and the resultant values are summarized in Table 2. The linear correlations are found to be excellent for reactions with all pprd-like ligands. The data in Table 2 quantitatively evaluate the relative affinity of the pprd ligands towards bpV, which confirm the assignments of the $^{51}V$ NMR spectra, as shown in Fig. 8, that **1** binds to bpV in two different ways and all other ligands bind in one way with the affinity trend of **1** ≈ **3** > **2** > **4** > **5**.

### Coordination mechanisms between bpV and the pprd-like ligands

In order to explore the coordination mechanisms, the bpV interactions with a series of pyridine-like or pyrimidine-like ligands, which are the building blocks of pprd, have been studied systematically and used as references. When 1 equivalent of pyridine-like or pyrimidine-like ligands were added to the bpV solutions, the peak areas of bpV decreased and new peaks appeared. As shown in Fig. 10, the peak at −710 ppm is assigned to $[OV(O_2)_2(Py)]^-$ for the pyridine (Py) ligand, −749 ppm is assigned to $[OV(O_2)_2(bipy)]^-$ for bipy, −709 ppm is assigned to $[OV(O_2)_2(2\text{-Me-Py})]^-$ for 2-methylpyridine (2-Me-Py), −700 ppm is assigned to $[OV(O_2)_2(Pym)]^-$ for pyrimidine (Pym) and −704 ppm is assigned to $[OV(O_2)_2(4\text{-Me-Pym})]^-$ for 4-methylpyrimidine (4-Me-Pym). The small new peaks at −732, −749 and −755 ppm can be assigned to $[HV_2O_3(O_2)_4]^{3-}$ according to the literature.[16] Importantly, based on the decreasing ratio of the bpV peak areas upon coordination, the relative affinity of the ligands towards bpV can be deduced as bipy > Py > Pym ≈ 4-Me-Pym > 2-Me-Py.

The coordination modes between bpV and the pyridine-like or pyrimidine-like ligands are summarized in Scheme 3. The above experimental results demonstrate that: (1) for a pyridine ligand with *ortho* substitution, coordination to bpV is permissive as shown in **10a–c** in Scheme 3. If the substitution group is also a coordination group, chelate effect enhances the stability of the complex, *e.g.* as in **10c** when the ligand is bipy; whereas steric effects weaken the coordination interaction, *e.g.* as in **10b** when

 

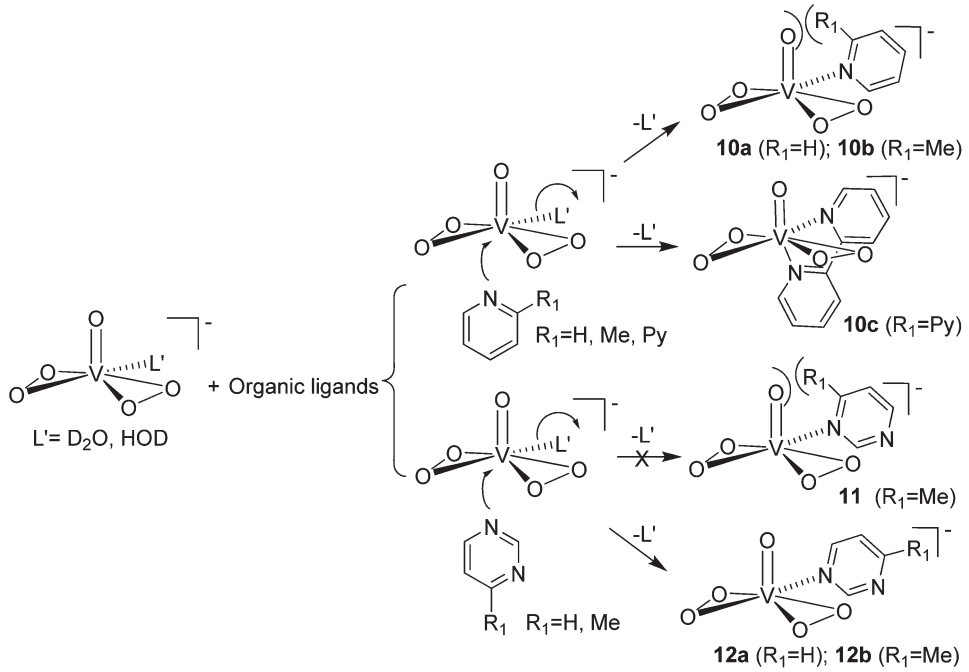


**Scheme 3** The coordination modes between bpV and the pyridine-like or pyrimidine-like ligands. '×' indicates a not allowed route. ')(' indicates a steric interaction.

the substituent is Me. Hence the coordination affinity is bipy > Py > 2-Me-Py. (2) Pym is a weaker coordination ligand than Py, which discourages coordination with the N3 atom for a substituted Pym (*e.g.* **11**). Coordination with N1 is allowed (*e.g.* **12a** and **12b**) as this places the substitution group in the *para* position, which minimizes the steric interaction. Hence the coordination affinity is Py > Pym ≈ 4-Me-Pym.

Conte and co-workers suggested that, for a neutral monodentate ligand, there exist two possible coordination modes for the ligand binding to $[OV(O_2)_2]^-$: the ligand can either lie in the equatorial plane of the peroxide oxygens or be on the axis *trans* to the oxido group.[17] Their *ab initio* calculations indicated that the former is more favorable in energy than the latter. This understanding can be extended to understand the coordination mechanisms of the pprd-like ligands to bpV studied here. We suppose that, for the pprd-like bidentate ligands, the interaction process may be artificially decomposed to two steps (see Scheme 4). Since the coordination ability of pyridine is stronger than that of pyrimidine, the pyridine building block is expected to occupy the favorable equatorial position first to form a hexa-coordinated **Intermediate A**. This is then followed by binding of the pyrimidine building block to the metal center epaxially to form the final hepta-coordinated peroxidovanadate. This (*i.e.*, **Route A** in Scheme 4) actually gives the main product of the coordination mode of **Isomer A** for pprd (**1**). The minor product of the coordination mode, **Isomer B**, is thus formed *via* the alternative path (*i.e.*, **Route B** in Scheme 4), which is less energetically favorable, where the pyrimidine building block occupies the equatorial position first followed by the binding of the pyridine building block to the metal from the axial position. For other pprd-like ligands (**2–7**), the substitution effects from $R_1$ and $R_2$ have to be taken into account to understand the stability of the biperoxidovanadate complexes.

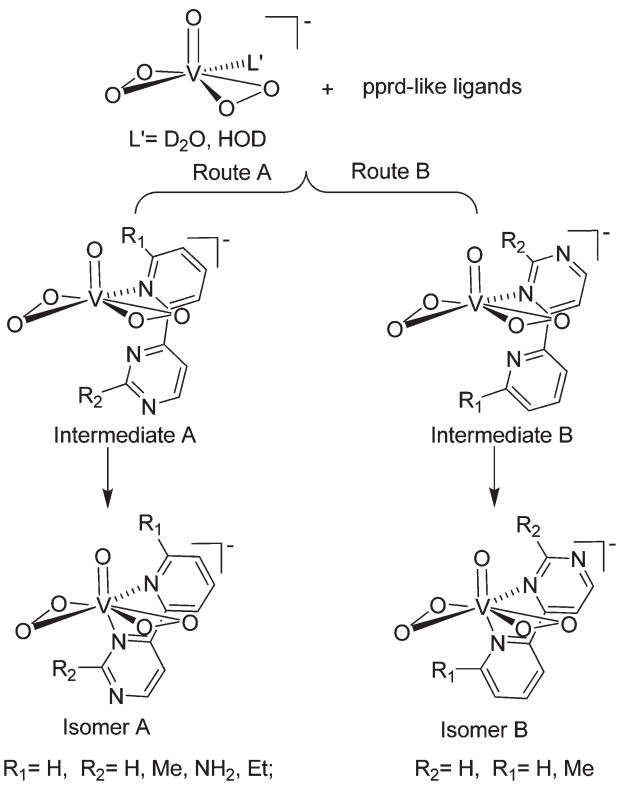


**Scheme 4** The possible interaction modes between bpV and the pprd-like ligands in solution.

It is clear that any ligand with a substituent in the *ortho* position of pyrimidine (*i.e.*, $R_2$ in Scheme 4) can not form a peroxidovanadate complex *via* **Route B** due to the steric repulsion.

This excludes the existence of any **type B** isomers for the pprd-like ligands of **2–4**, **6** and **7** with $R_2$ other than H. Hence, in addition to **1**, only 6′-Me-pprd (**5**) can survive as the **type B** isomer.

It is interesting to predict whether **5** can also lead to the formation of a **type A** isomer. We know that even though pyridine can bind strongly to bpV, an *ortho* substitution with methyl will diminish its binding affinity (Fig. 10(b) *vs*. (d)). 6′-Me-pprd (**5**) can be viewed as a pyridine with two *ortho* substitutions, which eliminate its possibility to bind to bpV in the equatorial position. Hence, 6′-Me-pprd (**5**) can only form the type **B** isomer. Indeed, only one coordination mode is observable, as shown in Fig. 8(e).

Similarly, 2-Me-6′-Me-pprd (**6**) and 2-$NH_2$-6′-Me-pprd (**7**) can also be viewed as pyridines with two *ortho* substitutions. They will neither form the type **A** isomer nor the type **B** isomer. Hence, ligands **6** and **7** have no binding affinity to bpV as observed experimentally (see Fig. 8(f) and 8(g)).

Ligand 2-Me-pprd (**2**), 2-$NH_2$-pprd (**3**) or 2-Et-pprd (**4**) is pyridine with one *ortho* substituent that can form a chelating complex (see **10a–c** in Scheme 3). Hence, forming the type **A** isomer is permissive for these ligands. If the steric effects of $R_2$ are taken into account, the ligand binding affinity to bpV should follow the trend of **1** > **2** > **4**. The electronic nature of the –$NH_2$ makes it different from –Me and –Et. For the 2-$NH_2$-pprd (**3**) ligand, besides the steric effect, there also exist hydrogen bonding interactions. As indicated by the distances of the H in –$NH_2$ to O4 (2.432 Å) or O2 (2.531 Å) in crystal **9** in Fig. 1, the hydrogen bond interactions are strong enough to overcome its otherwise steric repulsion. This helps to improve the complex stability and gives rise to similar binding affinities towards bpV for **1** and **3**.

These provide a clear understanding of the coordination mechanisms between bpV and the pprd-like ligands in solution, which suggest that the ligand binding affinities follow the trend of **1** ≈ **3** > **2** > **4** > **5** with **6** and **7** having no affinity.

## Conclusion

In this paper, several NMR experimental techniques were employed to study the interactions between a biperoxidovanadate complex (bpV) and a series of 4-(pyridin-2-yl)pyrimidine (abbreviated to pprd)-like ligands in a 0.15 mol $L^{-1}$ NaCl $D_2O$ solution. The relative affinities of the pprd-like ligands are **1** ≈ **3** > **2** > **4** > **5** with **6** and **7** having no affinity. When the ligand is pprd, a pair of isomers (**Isomer A** and **B**) are observed in the aqueous solution, which are attributed to the different types of coordination between the vanadium atom and the ligands, while the crystal structure of **8** has the same coordination structure as **Isomer A**. For substituted pprd ligands, however, only one type of structure (**Isomer A** or **Isomer B** ) is observed in solution. These results demonstrate that, when the aromatic ring has a substituted group, both the steric effect (from the alkyl) and the hydrogen bonding (from the amino) can affect the reaction equilibrium to prevent the appearance of either **Isomer B** in solution for the ligands **2**, **3** and **4**, or **Isomer A** in solution for the ligand **5**.

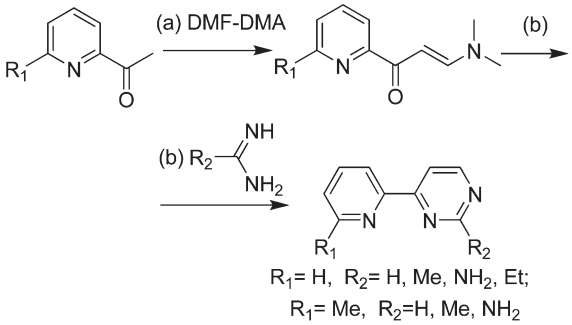


**Scheme 5** The synthetic route toward pprd-like ligands. (a) *N*,*N*-Dimethylformamide dimethylacetal (DMF–DMA), 110 °C; (b) $R_2C(NH)NH_2$, NaOEt, 65–85 °C.

## Experimental section

### Materials and preparation

The compounds $NH_4VO_3$, $NaVO_3$, $H_2O_2$ (30%), 4-(2-hydroxyethyl)-1-piperazineethanesulfonic acid (HEPES) and KCl were commercial products from Sinopharm Chemical Reagent Company and used without further purification. The pprd-like ligands were synthesized according to the method reported in the literature,[18] as shown in Scheme 5. The experimental procedures and spectroscopic data of these compounds are summarized in the ESI†.

To form the complex systems of $NaVO_3/H_2O_2$/L (L = **4**) or $NH_4VO_3$–$H_2O_2$–L (L = **1–3** or **5–7**), $NaVO_3$ or $NH_4VO_3$ and $H_2O_2$ were mixed first with a 1 : 5 molar ratio of the bpV solution and then the respective ligands were added to the solution. Unless otherwise stated, the total concentration of the vanadate species was 0.2 mol $L^{-1}$.

The biperoxidovanadate crystals were prepared by adding 10 mL $H_2O_2$ (30%, w/v, solution) and 1.17 g $NH_4VO_3$ to 50 mL distilled water. After the $NH_4VO_3$ was dissolved, 1.57 g pprd (**1**) or 1.72 g 2-$NH_2$-pprd (**3**) was added to the mixture. The mixture was stirred in an ice water bath at 273 K for 0.5–1 h. After this time, ethanol was added gradually until a precipitate appeared. The reaction mixture was then filtered and the solution was kept at 278–283 K for a week to crystallize. The crystals were filtered and washed with 2 mL cold water and 7 mL cold ethanol (3 times) and then dried on a filter paper. The isolated yield was 60–80% based on the vanadate.

### Crystal structure determination

Determination of the unit cell and data collection for the biperoxidovanadate compounds were performed on a R-AXIS SPIDER-R (for $NH_4[OV(O_2)_2(pprd)]\cdot 2H_2O$, **8**) or Bruker SMART CCD (for $NH_4[OV(O_2)_2(2\text{-}NH_2\text{-}pprd)]\cdot 3H_2O$, **9**) diffractometer at 173 K. Crystal data and details of the data collection and refinement are shown in Table 3. The structures were solved using a direct method as implemented in the program SHELXS97. The non-hydrogen atoms were refined using the full-matrix least-square procedure on $F^2$. Anisotropic displacement parameters were assigned to the non-hydrogen atoms. CCDC 801329 and 801327 contain the crystallographic data for **8** and **9**, respectively.

 

**Table 3** Experimental crystal data and structure refinement parameters for $NH_4[OV(O_2)_2(pprd)]\cdot 2H_2O$ (**8**) and $NH_4[OV(O_2)_2(2\text{-}NH_2\text{-}pprd)]\cdot 3H_2O$ (**9**)

| Compound reference | **8** | **9** |
|---|---|---|
| Chemical formula | $C_9H_{11}N_4O_7V$ | $C_9H_{18}N_5O_8V$ |
| Formula mass | 338.16 | 375.22 |
| Crystal system | Orthorhombic | Monoclinic |
| $a$/Å | 12.9276(14) | 7.2721(16) |
| $b$/Å | 6.9044(6) | 16.236(4) |
| $c$/Å | 15.8482(13) | 12.963(3) |
| $\alpha$/° | 90.00 | 90.00 |
| $\beta$/° | 90.00 | 98.622(4) |
| $\gamma$/° | 90.00 | 90.00 |
| Unit cell volume/Å$^3$ | 1414.6(2) | 1513.2(6) |
| Temperature/K | 173(2) | 173(2) |
| Space group | *Pnma* | *P*21/*c* |
| No. of formula units per unit cell, $Z$ | 4 | 4 |
| No. of reflections measured | 3638 | 12 607 |
| No. of independent reflections | 1363 | 3537 |
| $R_{int}$ | 0.0335 | 0.0444 |
| Final $R_1$ values ($I > 2\sigma(I)$) | 0.0408 | 0.0916 |
| Final w$R(F^2)$ values ($I > 2\sigma(I)$) | 0.0999 | 0.2173 |
| Final $R_1$ values (all data) | 0.0570 | 0.0972 |
| Final w$R(F^2)$ values (all data) | 0.1037 | 0.2211 |
| CCDC number | 801329 | 801327 |

### Spectroscopic measurements

Room temperature solid-state NMR experiments were performed on a 300 MHz Bruker DMX NMR spectrometer, operating at 78.8 MHz for $^{51}$V NMR and 75.5 MHz for $^{13}$C NMR. The $^{51}$V chemical shifts were referenced to $VOCl_3$, while the $^{13}$C chemical shifts were referenced to the carbonyl carbon of glycine, which, in turn, is 173.2 ppm with respect to that of tetramethylsilane. IR spectra were recorded on a Perkin–Elmer spectrometer (Spectrum One).

The solution NMR spectra were recorded on a 500 MHz Bruker AV II NMR spectrometer, operating at 500.13 MHz for $^1$H NMR, 125.77 MHz for $^{13}$C NMR and 131.47 MHz for $^{51}$V NMR. DSS (3-(trimethylsilyl)-propanesulfonic acid sodium salt) was used as an internal reference for $^1$H and $^{13}$C chemical shifts. $^{51}$V chemical shifts were measured relative to the external standard $VOCl_3$ with the upfield shifts considered as negative values. The signal-to-noise ratios were improved by a line-broadening factor of 2 Hz and 10 Hz in the Fourier transformation of all $^{13}$C and $^{51}$V spectra. In the NMR experiments, an ionic medium, 0.15 mol L$^{-1}$ NaCl $D_2O$, was chosen in order to represent physiological conditions. The temperature was generally 20 °C, while, in the variable temperature NMR, it varied from 20 °C to 40 °C at steps of 5 °C.

The equilibrium constants for coordination between bpV and the pprd-like ligands were measured *via* NMR studies according to Tracey's method.[7] The main conditions of the experiments were: temperature 25 °C, 15.0 mmol L$^{-1}$ total vanadate, 0.6 mol L$^{-1}$ KCl, 20 mM HEPES buffer (pH 6.8) and variable amounts of the pprd-like ligands (0–6.0 mmol L$^{-1}$).

Detailed spectroscopic measurement results may be found in the ESI.†

## Acknowledgements

This work was supported by the National Natural Science Foundation of China (20803020, 20971041, 21172066, 51103122), the Ministry of Science and Technology (2011CB808505) and the Open Project Program of Key Laboratory of Theoretical Chemistry and Molecular Simulation of Ministry of Education (Hunan University of Science and Technology).

## References

1 (*a*) K. H. Thompson and C. Orvig, *Science*, 2003, **300**, 936–939; (*b*) K. H. Thompson and C. Orvig, *J. Inorg. Biochem.*, 2006, **100**, 1925–1935; (*c*) K. H. Thompson, J. H. McNeill and C. Orvig, *Chem. Rev.*, 1999, **99**, 2561–2572.
2 (*a*) D. C. Crans, J. J. Smee, E. Gaidamauskas and L. Yang, *Chem. Rev.*, 2004, **104**, 849–902; (*b*) D. C. Crans, A. D. Keramidas, S. S. Amin, O. P. Anderson and S. M. Miller, *J. Chem. Soc., Dalton Trans.*, 1997, 2799–2812.
3 D. C. Crans, A. D. Keramidas, H. Hoover-Litty, O. P. Anderson, M. M. Miller, L. M. Lemoine, S. Pleasic-Williams, M. Vandenberg, A. J. Rossomando and L. J. Sweet, *J. Am. Chem. Soc.*, 1997, **119**, 5447–5448.
4 A. Butler and J. V. Walker, *Chem. Rev.*, 1993, **93**, 1937–1944.
5 B. I. Posner, R. Faure, J. W. Burgess, A. P. Bevan, D. Lachance, G. Y. Zhang-Sund, I. G. Fantus, J. B. Ng, D. A. Hall, B. S. Lum and A. Shaver, *J. Biol. Chem.*, 1994, **269**, 4596–4604.
6 (*a*) J. H. Hwang, R. K. Larson and M. M. Abu-Omar, *Inorg. Chem.*, 2003, **42**, 7967–7977; (*b*) M. Sam, J. H. Hwang, G. Chanfreau and M. M. Abu-Omar, *Inorg. Chem.*, 2004, **43**, 8447–8455; (*c*) D. W. J. Kwong, O. Y. Chan, R. N. S. Wong, S. M. Musser, L. Vaca and S. I. Chan, *Inorg. Chem.*, 1997, **36**, 1276–1277.
7 (*a*) A. S. Tracey and J. S. Jaswal, *Inorg. Chem.*, 1993, **32**, 4235–4243; (*b*) J. S. Jaswal and A. S. Tracey, *J. Am. Chem. Soc.*, 1993, **115**, 5600–5607.
8 (*a*) V. Conte, F. Di Furia and S. Moro, *Tetrahedron Lett.*, 1994, **35**, 7429–7432; (*b*) M. Andersson, V. Conte, F. Di Furia and S. Moro, *Tetrahedron Lett.*, 1995, **36**, 2675–2678; (*c*) V. Conte, F. Di Furia, S. Moro and S. Rabbolini, *J. Mol. Catal. A: Chem.*, 1996, **113**, 175–184; (*d*) V. Conte and B. Floris, *Inorg. Chim. Acta*, 2010, **363**, 1935–1946; (*e*) V. Conte, F. Fabbianesi, B. Floris, P. Galloni, D. Sordi, I. W. C. E. Arends, M. Bonchio, D. Rehder and D. Bogdal, *Pure Appl. Chem.*, 2009, **81**, 1265–1277.
9 (*a*) G. J. Colpas, B. J. Hamstra, J. W. Kampf and V. L. Pecoraro, *J. Am. Chem. Soc.*, 1994, **116**, 3627–3628; (*b*) G. J. Colpas, B. J. Hamstra, J. W. Kampf and V. L. Pecoraro, *J. Am. Chem. Soc.*, 1996, **118**, 3469–3478; (*c*) T. S. Smith and V. L. Pecoraro, *Inorg. Chem.*, 2002, **41**, 6754–6760; (*d*) G. Zampella, P. Fantucci, V. L. Pecoraro and L. De Gioia, *Inorg. Chem.*, 2006, **45**, 7133–7143.
10 A. Shaver, J. B. Ng, D. A. Hall, B. S. Lum and B. I. Posner, *Inorg. Chem.*, 1993, **32**, 3109–3113.
11 (*a*) X. Y. Yu, X. Xu and Z. Chen, *Int. J. Mass Spectrom.*, 2008, **269**, 138–144; (*b*) X. Y. Yu, S. H. Cai, X. Xu and Z. Chen, *Inorg. Chem.*, 2005, **44**, 6755–6762; (*c*) X. Y. Yu, S. H. Cai and Z. Chen, *J. Inorg. Biochem.*, 2005, **99**, 1945–1951; (*d*) X. Y. Yu, J. Zhang, S. H. Cai, P. G. Yi and Z. Chen, *Spectrochim. Acta, Part A*, 2009, **72**, 965–969; (*e*) B. R. Zeng, R. Q. Fu, S. H. Cai, J. Zhang and Z. Chen, *Inorg. Chim. Acta*, 2011, **365**, 119–126; (*f*) B. R. Zeng, R. Q. Fu, S. H. Cai and Z. Chen, *Inorg. Chem. Commun.*, 2009, **12**, 1259–1262.
12 (*a*) A. Gorzsas, I. Anderson and L. Pettersson, *J. Inorg. Biochem.*, 2009, **103**, 517–526; (*b*) L. Pettersson, I. Andersson and A. Gorzsas, *Coord. Chem. Rev.*, 2003, **237**, 77–87; (*c*) I. Andersson, A. Gorzsas and L. Pettersson, *Dalton Trans.*, 2004, 421–428; (*d*) H. Schmidt, I. Andersson, D. Rehder and L. Pettersson, *J. Inorg. Biochem.*, 2000, **80**, 149–151; (*e*) H. Schmidt, I. Andersson, D. Rehder and L. Pettersson, *Chem.–Eur. J.*, 2001, **7**, 251–257; (*f*) A. Gorzsas, I. Andersson and L. Pettersson, *Dalton Trans.*, 2003, 2503–2511; (*g*) M. Časný and D. Rehder, *Dalton Trans.*, 2004, 839–846.
13 (*a*) D. A. Beauchamp and S. J. Loeb, *Chem. Commun.*, 2002, 2484–2485; (*b*) M. Maekawa, S. Kitagawa, T. Kuroda-Sowa and M. Munakata, *Chem. Commun.*, 2006, 2161–2163; (*c*) M. Maekawa, H. Konaka, T. Minematsu, T. Kuroda-Sowa, M. Munakata and S. Kitagawa, *Chem. Commun.*, 2007, 5179–5181; (*d*) M. Maekawa, A. Nabei, T. Tominaga, K. Sugimoto, T. Minematsu, T. Okubo, T. Kuroda-Sowa, M. Munakata and S. Kitagawa, *Dalton Trans.*, 2009, 415–417.
14 (*a*) A. Shaver, D. A. Hall, J. B. Ng, A. M. Lebuis, R. C. Hynes and B. I. Posner, *Inorg. Chim. Acta*, 1995, **229**, 253–260; (*b*) P. Schwendt,

M. Ahmed and J. Marek, *Inorg. Chem. Commun.*, 2004, **7**, 631–633; (*c*) J. Tatiersky, P. Schwendt, J. Marek and M. Sivak, *New J. Chem.*, 2004, **28**, 127–133; (*d*) D. Begin, F. W. B. Einstein and J. Field, *Inorg. Chem.*, 1975, **14**, 1785–1790; (*e*) S. Helga and S. Rolf, *Acta Chem. Scand*, 1983, **A37**, 553–559.

15 (*a*) X. Y. Yu, R. H. Liu, H. L. Peng, H. W. Huang, X. F. Li, B. S. Zheng, P. G. Yi and Z. Chen, *Spectrochim. Acta, Part A*, 2010, **75**, 1095–1099; (*b*) X. Y. Yu, F. X. Yang, D. H. Ji, J. M. Zhou, R. H. Liu;, G. B. Li, X. F. Li, J. Chen, H. W. Huang and P. G. Yi, *Spectrochim. Acta, Part A*, 2010, **77**, 816–820; (*c*) X. Y. Yu, D. H. Ji, R. H. Liu, F. X. Yang, J. Xie, J. M. Zhou, X. F. Li and P. G. Yi, *J. Coord. Chem.*, 2010, **63**, 1555–1562; (*d*) R. J. Zeng, Z. X. Wang, X. F. Li, J. Xie and X. Y. Yu, *J. Coord. Chem.*, 2010, **63**, 498–504.

16 D. Rehder, T. Polenova and M. Bühl, *Ann. Rep. NMR Spectrosc.*, 2007, **62**, 50–114.

17 V. Conte, O. Bortolini, M. Carraro and S. Moro, *J. Inorg. Biochem.*, 2000, **80**, 41–49.

18 E. Bejan, H. Ait-Haddou, J. C. Daran and G. G. A. Balavoine, *Synthesis*, 1996, 1012–1018.



 